

Complete and Deterministic Bell state identification by two photon hyper-entanglement

M. Barbieri¹, G. Vallone², P. Mataloni¹ and F. De Martini¹

¹Dipartimento di Fisica dell'Università "La Sapienza" and Consorzio Nazionale Interuniversitario per le Scienze Fisiche della Materia, Roma, 00185 Italy

²Dipartimento di Fisica Teorica dell'Università di Torino and INFN - sezione di Torino - 10100 Italy

A complete and deterministic Bell-state measurement was realized by a simple linear optics experimental scheme which adopts 2-photon polarization-momentum hyper-entanglement. The scheme, which is based on the discrimination among the single photon Bell states of the hyper-entangled state, requires the adoption of standard single photon detectors. The four polarization Bell states have been measured with average fidelity $F = 0.889 \pm 0.010$ by using the linear momentum degree of freedom as the ancilla. The feasibility of the scheme has been characterized as a function of purity of momentum entanglement.

PACS numbers: 03.67.-a, 03.67.Hk, 42.65.Lm

In the domain of Quantum information (QI) the completion of most fundamental quantum communication protocols involving bipartite entanglement, such as quantum teleportation [1], quantum dense coding [2], entanglement swapping [3] and some important quantum cryptographic schemes [4] requires the complete and deterministic identification of the Bell states which form the orthogonal basis for the reference Hilbert space of the bipartite system.

In quantum optics, pairs of correlated photons are generated by spontaneous parametric down conversion (SPDC) in a nonlinear (NL) optical crystal slab by choosing suitably phase matching conditions. Photon qubits can be encoded in several accessible degrees of freedom, such as polarization [5, 6], linear and orbital momentum [7, 8], besides energy-time and time bin [9, 10]. In particular, the four orthogonal entangled Bell states, expressed in the logic basis 0, 1:

$$\begin{aligned} |\Phi^\pm\rangle &= \frac{1}{\sqrt{2}} (|0\rangle_A |0\rangle_B \pm |1\rangle_A |1\rangle_B), \\ |\Psi^\pm\rangle &= \frac{1}{\sqrt{2}} (|0\rangle_A |1\rangle_B \pm |1\rangle_A |0\rangle_B) \end{aligned} \quad (1)$$

form the complete maximally entangled basis of the Hilbert space $\mathcal{H}_A \otimes \mathcal{H}_B$ with $\dim(\mathcal{H}_A) = \dim(\mathcal{H}_B) = 2$. In the particular case of a photon polarization entangled state, 0 and 1 may correspond to the horizontal (H) and vertical (V) field polarization.

By standard linear methods, the discrimination of polarization Bell states can not be achieved by simply performing a single joint measurement on the two particles. Indeed, a reliable experimental scheme, capable to deterministically distinguish among the four entangled Bell states with 100% efficiency by using 2×2 entangled photon pairs and standard linear optics, doesn't exist and only a partial Bell state analysis with a maximum attainable value of 50% efficiency can be performed [11]. Recently, probabilistic complete Bell state analyzers for photonic quantum bits were demonstrated by using a controlled-Not (C-NOT) gate for photonic qubits [12].

The strategy adopted to overcome the intrinsic probabilistic character of any Bell analysis exploits further degrees of freedom in the entangled state as ancillas.

In fact, by two photons entangled in $N > 1$ degrees of freedom, namely hyper-entangled states, spanning the $2^N \times 2^N$ Hilbert space, a complete and deterministic Bell state analysis can be performed with standard linear optics [13, 14]. In the case of double entangled states ($N = 2$) it was shown that this operation can occur together with a C-NOT logic operation between the control and target degrees of freedom [14]. The experimental demonstration of a complete analysis of the four polarization entangled Bell states has been recently given by Schuck *et al.* [15] who used the polarization entanglement of two photons generated by a Type II NL crystal and the intrinsic time-energy entanglement occurring in the SPDC process. The measurement apparatus described in that work consisted of a sequence of three different steps which allowed to distinguish among the four polarization entangled states. By that scheme, a full deterministic analysis of all the photon pairs requires the adoption of photon number resolving detectors.

In this letter we demonstrate that a complete and deterministic analysis of the Bell states (1) can be performed by discriminating among the single photon Bell states of a polarization (π) - momentum (\mathbf{k}) hyper-entangled two-photon state, at the Alice (A) and Bob (B) sites. By our scheme the four Bell states $|\Phi^+\rangle$, $|\Phi^-\rangle$, $|\Psi^+\rangle$, $|\Psi^-\rangle$, have been analyzed with high fidelity and equal detection probabilities by a single step measurement apparatus and using single photon detectors. On this purpose we used the SPDC source of π - \mathbf{k} hyper-entangled two-photon states, based on a single Type I β -BaB₂O₄ (BBO) crystal, already described in other experiments (cfr. Fig. 1a) [16]. By this source the hyper-entangled state

$$\begin{aligned} |\Xi\rangle &= |Bell\rangle \otimes |\psi^+\rangle \\ &= |Bell\rangle \otimes \frac{1}{\sqrt{2}} (|a_1\rangle_A |b_2\rangle_B + |a_2\rangle_A |b_1\rangle_B) \end{aligned} \quad (2)$$

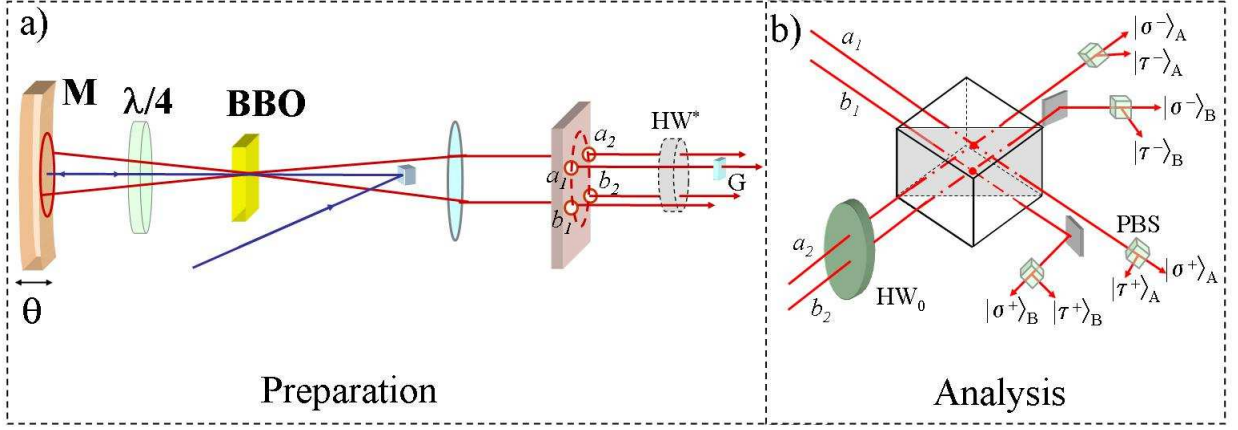


FIG. 1: a) Scheme of the hyper-entanglement source: the polarization entangled state $|\Phi\rangle = \frac{1}{\sqrt{2}}(|H\rangle|H\rangle + e^{i\theta}|V\rangle|V\rangle)$ comes from the superposition of the degenerate cones of a type-I BBO crystal. The basic elements of the source are: [i] a spherical mirror M , reflecting both the parametric radiation or the pump beam, whose micrometric displacement allows to control the state phase θ ($\theta = 0, \pi$). [ii] a $\lambda/4$ waveplate, placed within the M -BBO path, which performs the $|H\rangle_A|H\rangle_B \rightarrow |V\rangle_A|V\rangle_B$ transformation on the two-photon state belonging to the left-cone. [iii] a positive lens which transforms the conical parametric emission of the crystal into a cylindrical one. Mode selection is performed by a four hole mask. The $\lambda/2$ waveplate HW^* intercepting modes a_2, b_2 performs the $|\Phi^\pm\rangle \rightarrow |\Psi^\pm\rangle$ transformation, the glass plate G sets the phase of the momentum state. b) Scheme of the Bell state analyzer (see text for details).

is generated over two spatial mode sets, namely $a_1 - a_2$ and $b_1 - b_2$, belonging to the BBO emission cone and corresponding to the Alice and Bob site, respectively [16]. In the above expression the state $|Bell\rangle$ represents either one of the two-photon polarization Bell states, $|\Phi^\pm\rangle = \frac{1}{\sqrt{2}}(|H\rangle_A|H\rangle_B \pm |V\rangle_A|V\rangle_B)$, $|\Psi^\pm\rangle = \frac{1}{\sqrt{2}}(|H\rangle_A|V\rangle_B \pm |V\rangle_A|H\rangle_B)$. The parametric source, which allows to finely control the phase of the states, generates the entangled states $|\Phi^\pm\rangle$ [6]. Furthermore, the insertion of a zero-order $\lambda/2$ waveplate (wp) intercepting the modes a_2, b_2 (HW^* in Fig. 1a) allows to transform the state $|\Phi^+\rangle$ in $|\Psi^+\rangle$, while the transformation $|\Phi^-\rangle \rightarrow |\Psi^-\rangle$ is accompanied by a π phase shift on the momentum entangled state, $|\psi^+\rangle \rightarrow |\psi^-\rangle$. As a consequence, in order to generate $|\Psi^-\rangle \otimes |\psi^+\rangle$, we need to compensate this phase shift by suitable tilting of a thin glass plate inserted on mode a_1 (Fig. 1a). The nonlocal character of the hyper-entangled state $|\Xi\rangle$ generated by this source was recently demonstrated by two different

experiments, the All Versus Nothing (AVN) test [17] and the Bell's inequalities violation of local realism with two degrees of freedom [18].

By the present method, we are able to discriminate among the four possibility $|\Phi^+\rangle, |\Phi^-\rangle, |\Psi^+\rangle, |\Psi^-\rangle$, by using the single photon Bell basis:

$$\begin{aligned}
 |\sigma^\pm\rangle_A &= \frac{1}{\sqrt{2}}[|H\rangle|a_1\rangle_A \pm |V\rangle|a_2\rangle_A], \\
 |\sigma^\pm\rangle_B &= \frac{1}{\sqrt{2}}[|H\rangle|b_1\rangle_B \pm |V\rangle|b_2\rangle_B], \\
 |\tau^\pm\rangle_A &= \frac{1}{\sqrt{2}}[|V\rangle|a_1\rangle_A \pm |H\rangle|a_2\rangle_A], \\
 |\tau^\pm\rangle_B &= \frac{1}{\sqrt{2}}[|V\rangle|b_1\rangle_B \pm |H\rangle|b_2\rangle_B],
 \end{aligned} \tag{3}$$

which allows to express the four possible states $|\Xi\rangle$ as

$$\begin{aligned}
 |\Phi^+\rangle \otimes |\psi^+\rangle &= \frac{1}{2} [|\sigma^+\rangle_A|\tau^+\rangle_B - |\sigma^-\rangle_A|\tau^-\rangle_B + |\tau^+\rangle_A|\sigma^+\rangle_B - |\tau^-\rangle_A|\sigma^-\rangle_B], \\
 |\Phi^-\rangle \otimes |\psi^+\rangle &= \frac{1}{2} [-|\sigma^+\rangle_A|\tau^-\rangle_B + |\sigma^-\rangle_A|\tau^+\rangle_B + |\tau^+\rangle_A|\sigma^-\rangle_B - |\tau^-\rangle_A|\sigma^+\rangle_B], \\
 |\Psi^+\rangle \otimes |\psi^+\rangle &= \frac{1}{2} [|\sigma^+\rangle_A|\sigma^+\rangle_B - |\sigma^-\rangle_A|\sigma^-\rangle_B + |\tau^+\rangle_A|\tau^+\rangle_B - |\tau^-\rangle_A|\tau^-\rangle_B], \\
 |\Psi^-\rangle \otimes |\psi^+\rangle &= \frac{1}{2} [-|\sigma^+\rangle_A|\sigma^-\rangle_B + |\sigma^-\rangle_A|\sigma^+\rangle_B + |\tau^+\rangle_A|\tau^-\rangle_B - |\tau^-\rangle_A|\tau^+\rangle_B].
 \end{aligned} \tag{4}$$

Our scheme adopts linear momentum entanglement as

the ancilla and polarization entanglement as the target.

It is equivalent to the one proposed by Walborn et al. [14], except for the change of roles between the momentum and polarization degrees of freedom in that case.

Concerning the experimental apparatus, the upper and lower modes $a_1 - a_2$ and $b_1 - b_2$, which corresponds respectively to the upper and lower side of the BBO emission cone, are spatially and temporally combined onto a 50% beam splitter (BS) by an interferometric apparatus, where a trombone mirror assembly allows fine delay adjustment Δx between the mode sets $a_1 - b_1$ and $a_2 - b_2$ [16]. Precisely, the analyzing apparatus is given by the BS which follows a 45° oriented $\lambda/2$ wp (HW_0), inserted on the $a_2 - b_2$ side in order to intercept both the Alice than Bob modes (Fig. 1b) [19].

We are then able to completely distinguish among the states (3), that are transformed by HW_0 as:

$$\begin{aligned}
 |\sigma^\pm\rangle_A &\xrightarrow{HW_0} |H\rangle \otimes \frac{1}{\sqrt{2}} [|a_1\rangle_A \pm |a_2\rangle_A], \\
 |\sigma^\pm\rangle_B &\xrightarrow{HW_0} |H\rangle \otimes \frac{1}{\sqrt{2}} [|b_1\rangle_B \pm |b_2\rangle_B], \\
 |\tau^\pm\rangle_A &\xrightarrow{HW_0} |V\rangle \otimes \frac{1}{\sqrt{2}} [|a_1\rangle_A \pm |a_2\rangle_A], \\
 |\tau^\pm\rangle_B &\xrightarrow{HW_0} |V\rangle \otimes \frac{1}{\sqrt{2}} [|b_1\rangle_B \pm |b_2\rangle_B].
 \end{aligned} \tag{5}$$

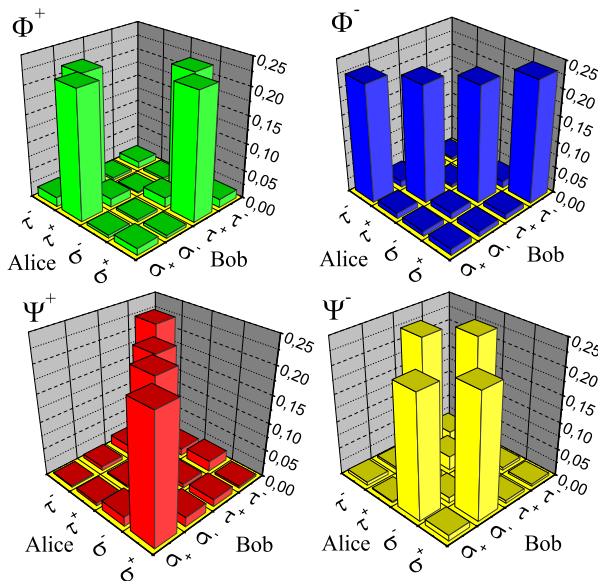


FIG. 2: Experimental coincidence frequencies showing the complete Bell state analysis of the polarization states $|\Phi^+\rangle$, $|\Phi^-\rangle$, $|\Psi^+\rangle$, $|\Psi^-\rangle$. Relative errors are typically 2% for the maxima, 5% for the other terms.

The BS discriminates between $|a_1\rangle_A + |a_2\rangle_A$ and $|a_1\rangle_A - |a_2\rangle_A$, $|b_1\rangle_B + |b_2\rangle_B$ and $|b_1\rangle_B - |b_2\rangle_B$ and polarization analysis on each BS output mode, performed

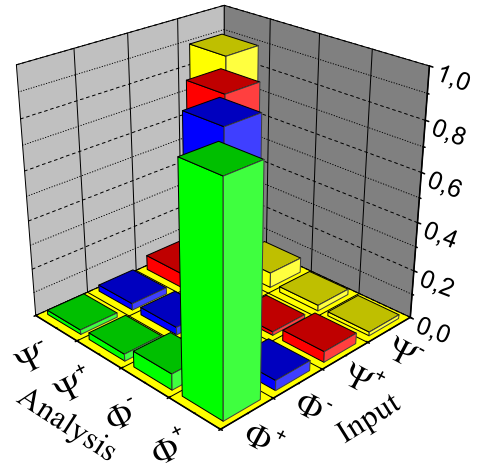


FIG. 3: Overall experimental fidelities obtained by the Bell state analyzer for each input Bell state. Relative errors are typically 2% for the maxima, 5% for the other terms.

by a polarizing beamsplitter (PBS), completes the single photon Bell state measurement [19]. Note that a completely deterministic Bell state analysis requires to detect the eight possible outputs of the apparatus (Fig. 1b). In our proof of principle experiment we used four avalanche single photon detectors, (mod. Perkin Elmer SPCM-AQR14) on the transmitted modes of the PBS 's. In the actual case the transmitted polarization is set by a further half-wave plate before each PBS .

The four 3-D histograms given in Fig. 2 show all the 16 possible combinations of the states (3) for either one of the states $|\Phi^+\rangle$, $|\Phi^-\rangle$, $|\Psi^+\rangle$, $|\Psi^-\rangle$ and demonstrate the successful implementation of the Bell state analyzer. Each datum was obtained in an acquisition time of 10 sec, while the typical count rate was $\simeq 1000 \text{ sec}^{-1}$ for each maximum measurement. The overall input-output histogram shown in Fig. 3 clearly indicates the high efficiency of the analysis performed by our scheme. The achieved fidelities of each Bell-state analysis are $F_{|\Phi^+\rangle} = 0.886 \pm 0.018$, $F_{|\Phi^-\rangle} = 0.895 \pm 0.018$, $F_{|\Psi^+\rangle} = 0.877 \pm 0.018$, $F_{|\Psi^-\rangle} = 0.899 \pm 0.018$, with an average value of 0.889 ± 0.010 . Notice that the single step measurement apparatus allows to identify the four Bell state with almost the same fidelity. The noise contribution due to the unexpected coincidences is partially caused by the non perfect purity of the polarization input state and partially due to imperfections of the analysis set-up, e.g. mode mismatch on BS .

To test the feasibility of the Bell state analyzer realized by our scheme, we measured the output of the analyzer when the state $|\Psi^+\rangle$ is injected, while introducing noise in a controlled way in the ancilla state $|\psi^+\rangle$. This was performed by varying the value of Δx in the interferometric apparatus. The experimental output fidelities,

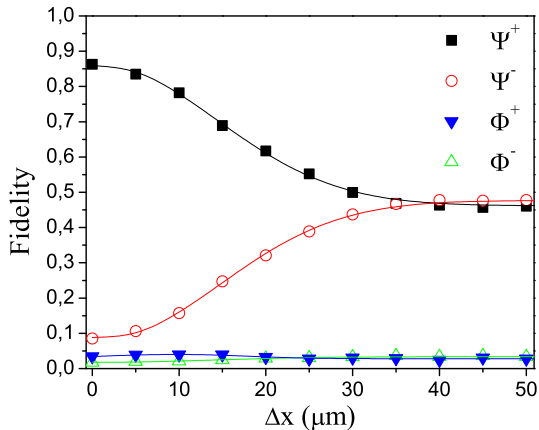


FIG. 4: Output fidelities of the states $|\Phi^+\rangle$, $|\Phi^-\rangle$, $|\Psi^+\rangle$, $|\Psi^-\rangle$, vs. the path length difference Δx in the interferometric apparatus (Input state: $|\Psi^+\rangle$). Error bars are smaller than the corresponding experimental points.

shown in Fig. 4, indicate, as expected, that $|\Psi^+\rangle$ and $|\Psi^-\rangle$ can not be discriminated when $\Delta x > l_{coh}$, the coherence length of the down converted photons imposed by the $\Delta\lambda = 6\text{nm}$ interference filters before the detectors. The results of Fig. 4 demonstrate that a still efficient Bell state analysis, with $F_{|\Psi^+\rangle} \geq 0.75$, may be performed

even with a partially degraded ancilla state. Similar results are expected when the input polarization entangled state is not pure.

We have presented in this letter a linear optical scheme based on two photon hyper-entanglement which allows to perform in a deterministic way the simultaneous measurement of the four polarization Bell states by using standard single photon detectors. By virtue of the simplicity of the measurement procedure and of the high fidelity experimentally attained, the present Bell state analyzer (Fig.1b) may be applied to any source able to produce polarization-momentum entangled photons [5, 16, 20] and could be useful for the realization of QI protocols, in particular dense coding and quantum key distribution. Precisely, the implementation of cryptographic schemes with qudits up to $d = 4$ (ququads) requiring 5 mutually unbiased bases and the consequent Bell state measurement can be efficiently performed by adopting the method described in the present work [21]. Indeed, it has been shown that these systems are more robust against specific classes of eavesdropping attacks [8].

Thanks are due to Serge Massar for useful discussions. This work was supported by the FIRB 2001 (*Realization of Quantum Teleportation and Quantum Cloning by the Optical Parametric Squeezing Process*) and PRIN 2005 (*New perspectives in entanglement and hyper-entanglement generation and manipulation*) of MIUR (Italy).

-
- [1] C. H. Bennett *et al.*, *Phys. Rev. Lett.* **70**, 1895 (1993).
[2] C. H. Bennett and S. J. Wiesner, *Phys. Rev. Lett.* **69**, 2881 (1992).
[3] T. Jennewein, G. Weihs, J. W. Pan, and A. Zeilinger, *Phys. Rev. Lett.* **88**, 017903 (2002); F. Sciarrino, E. Lombardi, G. Milani, and F. De Martini, *Phys. Rev. A* **66**, 024309 (2002).
[4] A. Ekert, *Nature* **358**, 14 (1992); N. Gisin, G. Ribordy, W. Tittel, and H. Zbinden, *Rev. Mod. Phys.* **74**, 145 (2002).
[5] P. G. Kwiat *et al.*, *Phys. Rev. Lett.* **75**, 4337 (1995); P. G. Kwiat, E. Waks, A. G. White, I. Appelbaum and P. H. Eberhard, *Phys. Rev. A* **60**, R773 (1999).
[6] C. Cinelli, G. Di Nepi, F. De Martini, M. Barbieri, and P. Mataloni, *Phys. Rev. A* **70**, 022321 (2004).
[7] J.G.Rarity, P.R.Tapster, *Phys. Rev. Lett.* **64**, 2495 (1990).
[8] N. Langford *et al.*, *Phys. Rev. Lett.* **93**, 053601 (2004).
[9] J. D. Franson, *Phys. Rev. Lett.* **62**, 2205 (1989).
[10] J. Brendel *et al.*, *Phys. Rev. Lett.* **82**, 2594 (1999).
[11] N. Lütkenhaus, J. Calsamiglia, and K.-A. Suominen, *Phys. Rev. A* **59**, 3295 (1999); J. Calsamiglia and N. Lütkenhaus, *Appl. Phys. B* **72**, 67 (2001).
[12] J. L. O'Brien *et al.*, *Phys. Rev. Lett.* **93**, 080502 (2004); Z. Zhao *et al.*, *Phys. Rev. Lett.* **94**, 030501 (2005); P. Walther and A. Zeilinger, *Phys. Rev. A* **72**, 010302(R) (2005).
[13] P. G. Kwiat and H. Weinfurter, *Phys. Rev. A*, **58**, R2623 (1998).
[14] S. P. Walborn, S. Pàdua and C. H. Monken, *Phys. Rev. A* **68**, 042313 (2003).
[15] C. Schuck, G. Huber, C. Kurtsiefer, and H. Weinfurter, *Phys. Rev. Lett.* **96**, 190501 (2006).
[16] M. Barbieri *et al.*, *Phys. Rev. A* **72**, 052110 (2005).
[17] C. Cinelli *et al.*, *Phys. Rev. Lett.* **95**, 240405 (2005).
[18] M. Barbieri *et al.*, "Enhancing the Violation of the Einstein-Podolsky-Rosen Local Realism by Quantum Hyper-entanglement", *quant-ph* 0608157, to appear on *Phys. Rev. Lett.*
[19] D. Boschi, S. Branca, F. De Martini, L. Hardy, S. Popescu, *Phys. Rev. Lett.* **80**, 1121 (1998).
[20] T. Yang *et al.*, *Phys. Rev. Lett.* **95**, 240406 (2005).
[21] G. M. D'Ariano, P. Mataloni and M. F. Sacchi *Phys. Rev. A* **71**, 062337 (2005).